Hindawi
International Journal of Aerospace Engineering
Volume 2018, Article ID 4126807, 15 pages
https://doi.org/10.1155/2018/4126807

Research Article

Cooperative Intercept Guidance of Multiple Aircraft with a Lure Role Included

Shuai Zhang,[1] **Yang Guo**,[1,2] **and Shicheng Wang**[1]

[1]*Xi'an Research Institute of Hi-Tech, Xi'an 710025, China*
[2]*Science and Technology on Electro-optical Control Laboratory, Luoyang 741000, China*

Correspondence should be addressed to Yang Guo; guoyang820@foxmail.com

Received 4 September 2017; Revised 17 January 2018; Accepted 21 January 2018; Published 10 April 2018

Academic Editor: Franco Bernelli-Zazzera

When threatened by a pursuer, an evading aircraft launches two defenders to accomplish a cooperative evasion, constituting a four-aircraft interception engagement. Under the assumption that the pursuing aircraft adopts the augmented proportional guidance law and first-order dynamics, a cooperative intercept mathematical model with an intercept angle constraint is established, allowing for the cooperative maneuvering of the evader. Based on the differential linear matrix inequality (DLMI), a controller design method of input and output finite time stability (IO-FTS) is proposed and applied to the aircraft's cooperative intercept scenario. A cooperation performance analysis is carried out for two cases: (1) two defenders intercept the pursuer with various intercept angle constraints, and (2) the evader acts in a lure role to cooperate with two defenders. The simulation results indicate that the proposed method of controller design has the ability to guarantee that the two defenders intercept the pursuer at the preassigned intercept angles. The cooperative intercept scenario with a lure role is shown to be a very effective method for reducing the maximum required acceleration for defenders, which confirms the availability and advantage of cooperation. The strong adaptability and robustness of the cooperative guidance law with respect to various initial launch conditions is also verified.

1. Introduction

A lone wolf cannot defeat a lion, but a group of wolves can easily contend against a lion, the reason for which is that the explicit division of labor, coordinated in cooperation, makes wolves much more powerful. There is an analogous case in an interception confrontation between multiple aircraft in which cooperation is also particularly important. The multiple-aircraft cooperative intercept scenario has become a subject of great interest in recent years. This paper addresses the tactics of cooperative defense in an engagement between four aircraft: an evader, two defenders, and a pursuer. For simplicity, the participants in this scenario are described by the terms Evader, Defender 1, Defender 2, and Pursuer, as shown in Figure 1. In this scenario, Evader may be a manned or unmanned aircraft of high value, such as a ballistic missile, aerial aircraft, or rocket. When confronted with a homing Pursuer, Evader launches two Defenders to intercept the incoming threat, which forms the four-aircraft interception engagement. It is expected that Evader, Defender 1, and Defender 2 can present superior intercept performance and improve the evader's probability of survival through mutual cooperation. The survivability of Evader is mainly contingent on two pivotal components of the four-aircraft engagement: the cooperative intercept strategy of Defender 1 and Defender 2 with intercept angle constraints, and the maneuver strategy of Evader in cooperation with the Defenders. The Defenders are expected to achieve a better intercept performance (e.g., all-around intercept) by pursuing different intercept angles in cooperation with the maneuvers of Evader, in which Evader takes on the role of a lure [1, 2].

According to the different strategies and roles in multiple-aircraft cooperative engagement, the existing cooperative scenario generally can be classified into two modes: one is the cooperative scenario of different collaborative tasks and roles and the other is the cooperative scenario of the same collaborative tasks and roles. In the first category, the current research focuses on the evader-attacker-defender scenario (an evader, a pursuer, and a defender), which means that the evading aircraft carries a defensive missile (defender)

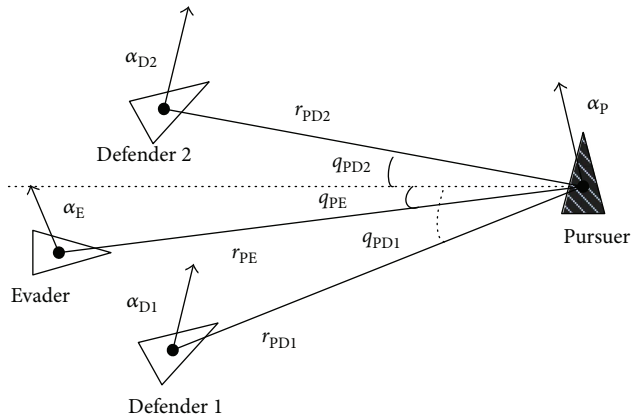

Figure 1: Schematic diagram of a four-aircraft engagement.

by itself, and the evader acts as a lure and the defender acts as an interception to cope with the incoming interceptor together. This scenario was proposed by Boyell [3, 4]. In recent years, this subject had been widely investigated. Shima [5] presented the optimal cooperative evasion and pursuit strategies for the evader and its defender missile on the condition that the pursuer use proportional navigation (PN), augmented proportional navigation (APN), and optimal guidance law (OGL). Prokopov and Shima [6] derived the optimal cooperation scheme for the evader and its defender missile based on a contrast analysis of three different linear quadratic cooperative strategies. Weiss et al. [7] proposed two minimum-effort guidance algorithms based on the required maximum miss distance for the attacker and the minimum required effort for target evasion. Additionally, Yamasaki and Balakrishnan [8] detailed a novel line-of-sight (LOS) geometry guidance law (referred to as triangle guidance) using a geometrical approach. The proposed guidance law ensures that the defender is located along the line segment between the evader and the pursuer. Ratnoo and Shima [9] derived a LOS geometry guidance law using a similar method. Guo et al. [10] proposed a cooperative guidance law for a three-aircraft engagement based on finite time theory in which the feedback controller was derived for cooperative evasion. In later research, Guo et al. [11] also derived maneuver control strategies for the evader based on finite time theory in the ballistic middle phase. This scenario involved the cooperative defense of evader and defender. The current research focuses on the optimal maneuvering strategy of the evader and defender to enable effective cooperative evasion.

The second cooperative scenario is developed on the basis of the traditional one-to-one interception. The assignment and role of each aircraft in the interception process are basically the same. The core idea of this scenario is the consensus of flight status or impact time under different flight conditions (e.g., communication delay, different topologies, and salvo attack with intercept angle constraint). Recently, the research focus lies in the many-to-one cooperative intercept scenario based on two-to-one (namely, attacker-attacker-target) scenario, which is very useful and critical for the cluster operations. For the attacker-attacker-target scenario, Shaferman and Shima [1, 2, 12] derived the optimal geometrical guidance law for explicit cooperation based on the optimal control theory. This two-to-one interception engagement was conducted by imposing a defender intercept angle without the cooperation of the evader in a lure role. Recently, Fonod and Shima [13, 14] proposed a cooperative guidance law via sharing the LOS angle between a team of aircraft. This method could enhance the intercept estimation performance by imposing an intercept angle, which relaxed the assumptions of constant acceleration and perfect information of the pursuer's actions considered in [1, 2, 12]. This cooperative scenario was an explicit extension of the traditional one-to-one intercept scenario, the focus of which was the design of a cooperative guidance law for attackers by improving the estimation of relative states. For the multiple-aircraft cooperative scenario, Du and Li [15] and Li et al. [16] propose a distributed delayed attitude control algorithm to ensure the attitude synchronization for flexible spacecraft when communication delay exists based on a multiagent system's theory. Zhang et al. [17] presented a distributed cooperative guidance law for the consensus of impact time with different communication networks. In summary, many scholars have conducted in-depth research on three-aircraft engagements and achieved some important results. However, the aforementioned research pays more attention to the optimal maneuvering of the attacker with the same role and performance. The cooperation between different roles in the engagement with an imposed intercept angle constraint in this scenario is rarely addressed [18–20].

A multiple-aircraft engagement is a typical finite time process: the intercept process must be completed within a finite time interval rather than over an infinite time period. The guidance command is also meaningful in a finite time interval [21–23]. Recently, many scholars have conducted related research to obtain a finite time convergent guidance law based on finite time theory in the terminal guidance phase [24–26]. The concept of a finite time theory was first proposed by Dorato in 1961 [27]. Recently, with the introduction of the effective solution of differential linear matrix inequality (DLMI), many scholars have turned their attention to the design of a finite time feedback controller. At this time, there are two main types of finite time stability concepts. The first is a theory proposed by Bernstein and Bhat [28] and extended to address nonautonomous systems by Hong et al. [29]. Du et al. [30, 31] and Xi et al. [32, 33] derived a finite-time cooperative control method that guarantees the state consensus in a finite time for a multiagent system. This finite time theory mainly relies on the Lyapunov stability analysis of nonlinear systems whose state trajectories converge to an equilibrium point in the finite time interval. The second finite time concept was proposed by Amato et al. [34], proposing the input and output finite time stability (IO-FTS) concept, which assumes that the output variables do not exceed a given threshold if the input variables are bounded in a finite time interval. Amato et al. [35–38] proposed sufficient conditions for the analysis of linear time-invariant systems in the IO-FTS concept via a feedback controller. The current paper focuses on the IO-FTS finite time theory proposed by Amato et al. because it is more practical in some cases of state saturation and input boundedness.

Inspired by the first scenario, we carried out the exploratory research based on the different roles in cooperation. As mentioned above, the aforementioned research focuses on the design of the optimal cooperative guidance law for a two-aircraft cooperative scenario based on optimal control theory, under the assumption that either the evader or defender possesses certain perfect information. Research into cooperative strategies between an evader and multiple defenders under intercept angles constraints is relatively lacking. An intercept scenario different than scenarios addressed in [12–14] is considered in this study based on the finite time theory: a pursuer, an evader, and multiple defenders, focusing on cooperative defense with different intercept angle constraints and evader lure role cooperation. The three-aircraft cooperative defense scenario (Evader, Defender 1, and Defender 2) is expected to achieve superior intercept performance. As the multiple-aircraft cooperative intercept issue is a typical finite time process, the current paper attempts to adopt the finite time theory to design a cooperative guidance law for different interception situations. Compared with the previous research, the current paper makes two main contributions: (1) the proposal of a cooperative intercept guidance law for two defenders with intercept angle constraints based on finite time theory and (2) the derivation of a multiple-aircraft cooperative interception strategy with an evader lure role to improve defender intercept performance.

The remainder of this paper is organized as follows. In Section 2, three types of multiple-aircraft cooperative intercept mathematical models are formulated, namely, (1) a cooperative interception model without the participation of the evader, (2) a cooperative interception model with the cooperation of the evader, and (3) a cooperative interception model with intercept angle constraints. In Section 3, we introduce the theory of input and output finite time stability (IO-FTS) and provide sufficient conditions for the input and output finite time stability of the linear time-variant (LTV) systems. A state feedback controller design method for the LTV system is proposed in the form of a differential linear matrix inequality based on finite time theory. In Section 4, a cooperative intercept performance analysis is carried out. Four intercept cases are simulated to verify the cooperative performance under intercept angle constraints and lure role cooperation. Section 5 presents concluding remarks.

2. Mathematical Model

A planar engagement between the four aircraft is considered. A schematic view of this engagement is shown in Figure 2. Variables associated with Evader, Defender 1, Defender 2, and Pursuer are denoted by the subscripts E, D1, D2, and P. Aircraft velocity is denoted by V, and normal acceleration is denoted by a. The ranges between Evader and Pursuer, Defender 1 and Pursuer, and Defender 2 and Pursuer are denoted by r_{PE}, r_{PD1}, and r_{PD2}, respectively. The LOS angles for Evader-to-Pursuer, Defender 1-to-Pursuer, and Defender 2-to-Pursuer are denoted by q_{PE}, q_{PD1}, and q_{PD2}, respectively. The rotation rate of LOS angles for Evader-to-Pursuer, Defender 1-to-Pursuer, and Defender 2-to-Pursuer is denoted by $\dot{q}_{PE}$, $\dot{q}_{PD1}$, and $\dot{q}_{PD2}$, respectively.

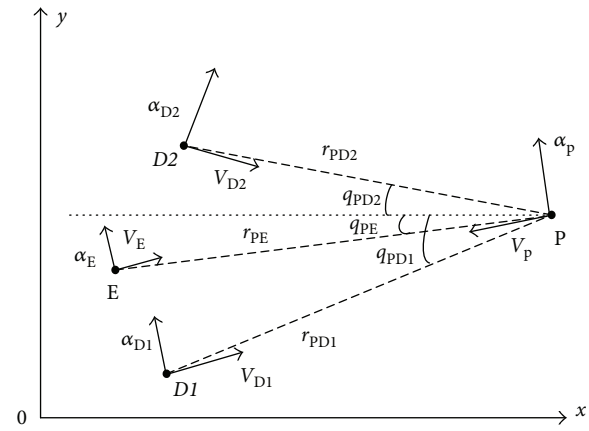

Figure 2: Schematic planar geometry of the four-aircraft engagement.

2.1. Kinematics and Dynamics

Assumption A. The four aircraft have first-order dynamics.

Assumption B. Pursuer adopts augmented proportional navigation.

Assumption C. Evader, Defender 1, and Defender 2 can share information with each other, and any delay is ignored.

According to the relative motion of the particles and the coordinate transformation, the relative motion equations between Evader and Pursuer can be derived as

$$\ddot{q}_{PE} = -2\frac{\dot{r}_{PE}}{r_{PE}}\dot{q}_{PE} + \frac{a_E - a_P}{r_{PE}}. \tag{1}$$

Similarly, the LOS rotation motions of Defender 1-Pursuer and Defender 2-Pursuer satisfy

$$\begin{aligned}\ddot{q}_{PD1} &= -2\frac{\dot{r}_{PD1}}{r_{PD1}}\dot{q}_{PD1} + \frac{a_{D1} - a_P}{r_{PD1}},\\ \ddot{q}_{PD2} &= -2\frac{\dot{r}_{PD2}}{r_{PD2}}\dot{q}_{PD2} + \frac{a_{D2} - a_P}{r_{D2}}.\end{aligned} \tag{2}$$

During the engagement, the velocities of the four agents are assumed to be constant, and intercept time can be approximated by

$$\begin{aligned}t_{fPE} &= r_{PE}\frac{0}{V_{PE}},\\ t_{fPD1} &= r_{PD1}\frac{0}{V_{PD1}},\\ t_{fPD2} &= r_{PD2}\frac{0}{V_{PD2}}.\end{aligned} \tag{3}$$

where $r_{PE}(0)$, $r_{PD1}(0)$, and $r_{PD2}(0)$ denote the initial range; and t_{fPE}, t_{fPD1}, and t_{fPD2} denote the total flight time of the Pursuer, Defender 1, and Defender 2, respectively.

Then the corresponding times-to-go t_{gPi} can be derived, where $i = \{E, D1, D2\}$.

$$\begin{aligned} t_{gPE} &= t_{fPE} - t, \\ t_{gPD1} &= t_{fPD1} - t, \\ t_{gPD2} &= t_{fPD2} - t. \end{aligned} \tag{4}$$

Obviously, the critical condition to ensure cooperative evasion is $t_{gPE} > t_{gPD1}$, $t_{gPE} > t_{gPD2}$. While the relative approaching velocities are positive values, the LOS angle rotation rate $\dot{q}$ needs to converge to zero in the terminal guidance stage to achieve the objective of accurate interception.

The dynamic equation can be expressed by (5), (6), (7), and (8) according to Assumption A.

$$\dot{a}_P = \frac{a_{PC} - a_P}{\tau_P}, \tag{5}$$

$$\dot{a}_E = \frac{a_{EC} - a_E}{\tau_E}, \tag{6}$$

$$\dot{a}_{D1} = \frac{a_{D1C} - a_{D1}}{\tau_{D1}}, \tag{7}$$

$$\dot{a}_{D2} = \frac{a_{D2C} - a_{D2}}{\tau_{D2}}, \tag{8}$$

where the variables τ_i denote the response time constant and the variables a_{iC} denote the normal acceleration command of vehicle i, where $i = \{E, D1, D2, P\}$.

According to Assumption B, the guidance law of the Pursuer is derived.

$$a_{PC} = NV_{PE}\dot{q}_{PE} + \frac{K}{2}a_E. \tag{9}$$

By (5) and (9), we have

$$\begin{aligned} \dot{a}_P &= \frac{1}{\tau_P}a_{PC} - \frac{1}{\tau_P}a_P = \frac{1}{\tau_P}\left(NV_{PE}\dot{q}_{PE} + \frac{K}{2}a_E\right) - \frac{1}{\tau_P}a_P \\ &= \frac{NV_{PE}}{\tau_P}\dot{q}_{PE} + \frac{K}{2\tau_P}a_E - \frac{1}{\tau_P}a_P, \end{aligned} \tag{10}$$

where N and K denote navigation parameters.

The relative movement of the four aircraft constitutes a system in which we describe the cooperative guidance law of Evader, Defender 1, and Defender 2. Therefore, the design of the acceleration commands a_{iC} forms the essence of the collaborative guidance law for $i = \{E, D1, D2\}$.

2.2. Evader Noncooperation with Defenders. In this case, Evader is considered to have a special mission that precludes its ability to freely maneuver in cooperation with Defender 1 and Defender 2 against Pursuer. The acceleration command of Evader is known by its defenders and is regarded as the external input vector $\mathbf{w}(t)$ of the four-aircraft engagement system. The acceleration commands of Defender 1 and Defender 2 are regarded as the control input vector $\mathbf{u}(t)$, while $\mathbf{x}(t)$ is regarded as the set of internal state variables.

Because we are concerned with the normal acceleration a_i, $i = \{E, D1, D2, P\}$ for each aircraft in the cooperative intercept process, as well as the relative LOS angle $[q_i \ \dot{q}_i]$, $i = \{PE, PD1, PD2\}$ among the four aircraft, the system state vector $\mathbf{x}(t)$ can be taken as

$$\mathbf{x}(t) = \begin{bmatrix} q_{PE} & q_{PD1} & q_{PD2} & \dot{q}_{PE} & \dot{q}_{PD1} & \dot{q}_{PD2} & a_P & a_E & a_{D1} & a_{D2} \end{bmatrix}^T. \tag{11}$$

According to (2), (3), (4), (5), (6), (7), (8), (9), and (10), the state equations of the system are deduced as

$$\dot{\mathbf{x}}(t) = \mathbf{A}(t)\mathbf{x}(t) + \mathbf{B}(t)\mathbf{u}(t) + \mathbf{G}(t)\mathbf{w}(t), \tag{12}$$

$$\mathbf{y}(t) = \mathbf{C}(t)\mathbf{x}(t), \tag{13}$$

where

$$\mathbf{A}(t) = \begin{bmatrix} 0 & 0 & 0 & 1 & 0 & 0 & 0 & 0 & 0 & 0 \\ 0 & 0 & 0 & 0 & 1 & 0 & 0 & 0 & 0 & 0 \\ 0 & 0 & 0 & 0 & 0 & 1 & 0 & 0 & 0 & 0 \\ 0 & 0 & 0 & \frac{-2}{t_{gPE}} & 0 & 0 & \frac{-1}{V_{PE}t_{gPE}} & \frac{1}{V_{PE}t_{gPE}} & 0 & 0 \\ 0 & 0 & 0 & 0 & \frac{-2}{t_{gPD1}} & 0 & \frac{-1}{V_{PD1}t_{gPD1}} & 0 & \frac{1}{V_{PD1}t_{gPD1}} & 0 \\ 0 & 0 & 0 & 0 & 0 & \frac{-2}{t_{gPD2}} & \frac{-1}{V_{PD2}t_{gPD2}} & 0 & 0 & \frac{-1}{V_{PD2}t_{gPD2}} \\ 0 & 0 & 0 & \frac{NV_{PE}}{\tau_P} & 0 & 0 & \frac{-1}{\tau_P} & \frac{K}{2\tau_P} & 0 & 0 \\ 0 & 0 & 0 & 0 & 0 & 0 & 0 & \frac{-1}{\tau_E} & 0 & 0 \\ 0 & 0 & 0 & 0 & 0 & 0 & 0 & 0 & \frac{-1}{\tau_{D1}} & 0 \\ 0 & 0 & 0 & 0 & 0 & 0 & 0 & 0 & 0 & \frac{-1}{\tau_{D2}} \end{bmatrix}, \tag{14}$$

in which $\mathbf{G}(t)$ denotes the corresponding transfer matrix of the external input.

Owing to the noncooperation between Evader and Defenders, we can only control the Defenders to intercept Pursuer, meaning the input vector $\mathbf{u}(t)$ can be expressed as

$$\mathbf{u}(t) = [a_{\mathrm{D1C}} a_{\mathrm{D2C}}]^{\mathrm{T}}. \tag{15}$$

The corresponding vectors $\mathbf{B}(t)$ and $\mathbf{G}(t)$ are expressed as

$$\mathbf{B}(t) = \begin{bmatrix} 0 & 0 & 0 & 0 & 0 & 0 & 0 & 0 & \frac{1}{\tau_{\mathrm{D1}}} & 0 \\ 0 & 0 & 0 & 0 & 0 & 0 & 0 & 0 & 0 & \frac{1}{\tau_{\mathrm{D2}}} \end{bmatrix}^{\mathrm{T}},$$
$$\mathbf{G}(t) = \begin{bmatrix} 0 & 0 & 0 & 0 & 0 & 0 & 0 & \frac{1}{\tau_{\mathrm{E}}} & 0 & 0 \end{bmatrix}^{\mathrm{T}}. \tag{16}$$

Setting $\mathbf{y}(t)$ as the evaluation output vector, and $\mathbf{y}(t) = \mathbf{C}(t)\mathbf{x}(t)$, the corresponding vector $\mathbf{C}(t)$ is expressed as

$$\mathbf{C}(t) = \begin{bmatrix} 0 & 1 & 0 & 0 & 0 & 0 & 0 & 0 & 0 & 0 \\ 0 & 0 & 1 & 0 & 0 & 0 & 0 & 0 & 0 & 0 \\ 0 & 0 & 0 & 0 & 1 & 0 & 0 & 0 & 0 & 0 \\ 0 & 0 & 0 & 0 & 0 & 1 & 0 & 0 & 0 & 0 \end{bmatrix}. \tag{17}$$

That is,

$$\mathbf{y}(t) = [\, q_{\mathrm{PD1}} \quad q_{\mathrm{PD2}} \quad \dot{q}_{\mathrm{PD1}} \quad \dot{q}_{\mathrm{PD2}} \,]^{\mathrm{T}}. \tag{18}$$

The system described by (12) and (13) is a typical time-varying system. In the four-aircraft interception engagement, we are concerned that the LOS angles q_{PD1} and q_{PD2} reach a designated intercept angle and that the LOS angle rotation rates $\dot{q}_{\mathrm{PD1}}$ and $\dot{q}_{\mathrm{PD2}}$ converge to zero in the finite time interval. In other words, the system evaluation output $\mathbf{y}(t)$ must meet the preassigned threshold in the finite time interval to provide accurate intercept.

2.3. Evader Cooperation with Defenders. In this case, the Evader is able to freely maneuver with Defender 1 and Defender 2 against Pursuer for improved intercept performance. It is then necessary to design the acceleration commands of Evader, Defender 1, and Defender 2 for cooperative evasion. At this point, according to (2), (3), (4), (5), (6), (7), (8), (9), and (10), the state equations of the system are deduced as

$$\dot{\mathbf{x}}(t) = \mathbf{A}(t)\mathbf{x}(t) + \mathbf{B}(t)\mathbf{u}(t) + \mathbf{G}(t)\mathbf{w}(t), \tag{19}$$

$$\mathbf{y}(t) = \mathbf{C}(t)\mathbf{x}(t), \tag{20}$$

where the acceleration commands of Evader, Defender 1, and Defender 2 constitute the input vector $\mathbf{u}(t)$ together, which implies that $\mathbf{u}(t)$ can be expressed as

$$\mathbf{u}(t) = [\, a_{\mathrm{EC}} \quad a_{\mathrm{D1C}} \quad a_{\mathrm{D2C}} \,]^{\mathrm{T}}. \tag{21}$$

The corresponding vector $\mathbf{B}(t)$ is expressed as

$$\mathbf{B}(t) = \begin{bmatrix} 0 & 0 & 0 & 0 & 0 & 0 & 0 & \frac{1}{\tau_{\mathrm{E}}} & 0 & 0 \\ 0 & 0 & 0 & 0 & 0 & 0 & 0 & 0 & \frac{1}{\tau_{\mathrm{D1}}} & 0 \\ 0 & 0 & 0 & 0 & 0 & 0 & 0 & 0 & 0 & \frac{1}{\tau_{\mathrm{D2}}} \end{bmatrix}^{\mathrm{T}}. \tag{22}$$

The external disturbance of the system can be regarded as the external input vector $\mathbf{w}(t)$. Matrices $\mathbf{A}(t)$ and $\mathbf{C}(t)$ are the same as those given in Section 2.2.

2.4. Intercept Model with Intercept Angle Constraint. When it is desired that Defender 1 and Defender 2 intercept Pursuer at designated intercept angles, an intercept model with angle constraints is considered. The state equations with an intercept angle constraint for the Defenders can be derived based on state equations (12), (13), (19), and (20), where the augmented state vector is denoted by $\bar{\mathbf{x}}(t)$, and $\bar{\mathbf{x}}(t) = \mathbf{x}(t) + \boldsymbol{\delta}$. The variable $\boldsymbol{\delta}$ can be regarded as the augmented vector of the system state, and $\boldsymbol{\delta} \in \mathbb{R}^{10}$. The augmented system state equations can then be rewritten as

$$\dot{\bar{\mathbf{x}}}(t) = \mathbf{A}_1(t)\bar{\mathbf{x}}(t) + \mathbf{B}(t)\mathbf{u}(t) + \mathbf{G}(t)\mathbf{w}(t), \tag{23}$$

$$\bar{\mathbf{y}}(t) = \mathbf{C}(t)\bar{\mathbf{x}}(t), \tag{24}$$

where $\mathbf{A}_1(t)$ denotes the augmented state matrix. By system equations (22) and (23), the cooperative guidance system equation with intercept angle constraint can be formulated.

For system equations (23) and (24), if the controller $\mathbf{u}(t)$ is designed in the form of state feedback, and $\mathbf{u}(t) = \mathbf{K}(t)\bar{\mathbf{x}}(t)$, the following system equations (25) and (26) can be derived in which $\mathbf{K}(t)$ denotes the state feedback matrix.

$$\dot{\bar{\mathbf{x}}}(t) = (\mathbf{A}_1(t) + \mathbf{B}(t)\mathbf{K}(t))\bar{\mathbf{x}}(t) + \mathbf{G}(t)\mathbf{w}(t), \tag{25}$$

$$\bar{\mathbf{y}}(t) = \mathbf{C}(t)\bar{\mathbf{x}}(t). \tag{26}$$

Remark 1. According to the state equations in Sections 2.2, 2.3, and 2.4, the essential role of the cooperative intercept guidance law is to design a state feedback controller $\mathbf{u}(t)$ in order to guarantee that the system output vector $\bar{\mathbf{y}}(t)$ meets the preassigned threshold in the finite time interval when the input vector $\mathbf{w}(t)$ is bounded. Specifically, one needs to design a state feedback controller $\mathbf{u}(t)$ that ensures that the LOS angles q_{PD1} and q_{PD2} converge to a preassigned intercept angle, and the LOS angle rotation rates $\dot{q}_{\mathrm{PD1}}$ and $\dot{q}_{\mathrm{PD2}}$ converge to zero in the finite time interval.

3. Cooperative Intercept Guidance Law

As mentioned above, the four-aircraft cooperative guidance process is a typical finite time process, and the cooperative intercept model established in Section 2 is also applied in the finite time interval. Therefore, in this section, we

introduce the input-output finite time stability theory for designing the controller $\mathbf{u}(t)$.

3.1. Input-Output Finite Time Stability Theory

Definition 1 (IO-FTS). Assume that the linear time-varying (LTV) system equations (27) and (28) are in the zero initial condition, namely, $\mathbf{x}(0) = 0$.

$$\dot{\mathbf{x}}(t) = \mathbf{A}(t)\mathbf{x}(t) + \mathbf{G}(t)\mathbf{w}(t), \tag{27}$$

$$\mathbf{y}(t) = \mathbf{C}(t)\mathbf{x}(t). \tag{28}$$

If the LTV system equations (27) and (28) satisfy the following condition,

$$\int_0^T \mathbf{w}^T(t)\mathbf{S}_w\mathbf{w}(t)dt \le 1 \Rightarrow \mathbf{y}^T(t)\mathbf{S}_y(t)\mathbf{y}(t) \le 1, \quad \forall t \in [0, T], \tag{29}$$

then the system equations (27) and (28) are said to possess input-output finite time stability with respect to $(T, \mathbf{S}_w, \mathbf{S}_y(\cdot))$. In Definition 1, $\mathbf{w}(t)$ denotes the external input vector, $\mathbf{y}(t)$ denotes the system output vector, $\mathbf{S}_w$ and $\mathbf{S}_y(t)$ denote a given measurement matrix and a measurement matrix function, respectively, and T denotes a given positive time scalar.

Remark 2. IO-FTS and Lyapunov bounded input-bounded output (BIBO) stability are two different concepts. The IO-FTS theory focuses on signals defined over a finite time interval. The input output signals of IO-FTS are all norm bounded by preassigned quantitative bounds. However, the Lyapunov BIBO stability focuses on the existence of the bounds of input and output signals during an infinite time period.

Remark 3. IO-FTS is usually defined in the zero initial condition, which is due to the fact that the initial conditions and input signals will affect both the system states and output simultaneously. However, the effects of system states and output can be superimposed for linear systems, such as the system described in (27) and (28). Moreover, controllers designed with zero initial conditions and nonzero initial conditions have a similar control effect.

Remark 4. The multiple-aircraft cooperative interception problem given above can also be described as follows: Given a positive time scalar t_f, a class of external input signals $\mathbf{w}(t)$ defined over $[0, t_f]$, and a positive definite matrix-valued function $\mathbf{S}_y(t)$, design the state feedback control law $\mathbf{u}(t)$ and $\mathbf{u}(t) = \mathbf{K}(t)\bar{\mathbf{x}}(t)$, where $\mathbf{K}(t)$ is a piecewise continuous matrix-valued function, such that the closed-loop system given in (25) and (26) satisfies output vector $\bar{\mathbf{y}}(t)$ stability in the finite time interval.

Theorem 1 (sufficient condition of IO-FTS) [35]. *If there exists a symmetric positive definite matrix-valued function $\mathbf{P}(t) \in R^{n\times n}$, such that the inequality equations (30), (31), and (32) hold,*

$$\dot{\mathbf{P}}(t) + \mathbf{A}^T(t)\mathbf{P}(t) + \mathbf{P}(t)\mathbf{A}(t) + \mathbf{P}(t)\mathbf{G}(t)\mathbf{S}_w^{-1}\mathbf{G}^T(t)\mathbf{P}(t) < 0, \tag{30}$$

$$\mathbf{P}(t) \ge \mathbf{C}^T(t)\mathbf{S}_y(t)\mathbf{C}(t), \tag{31}$$

$$t \in [0, T], \tag{32}$$

then the system given by (27) and (28) is described by IO-FTS with respect to $(T, \mathbf{S}_w, \mathbf{S}_y(t))$ in the finite time interval $[0, T]$.

3.2. Controller Design.

In order to design the cooperative guidance law for the four-aircraft engagement, we need to seek an appropriate state feedback controller $\mathbf{u}(t)$, such that the system given in (25) and (26) satisfies the input and output finite time stability. In this section, on the basis of Section 3, we propose a controller design method in the form of a differential linear matrix inequality.

Theorem 2 (IO-FTS state feedback controller design method). *If there exists a symmetric positive definite matrix-valued function $\mathbf{X}(t) \in R^{n\times n}$ and $\mathbf{L}(t) \in R^{r\times n}$, such that the inequality equations (33), (34), and (35) hold,*

$$\begin{bmatrix} -\dot{\mathbf{X}}(t) + \mathbf{X}(t)\mathbf{A}^T(t) + \mathbf{A}(t)\mathbf{X}(t) + \mathbf{B}(t)\mathbf{L}(t) + \mathbf{L}^T(t)\mathbf{B}^T(t) & \mathbf{G}(t) \\ \mathbf{G}^T(t) & -\mathbf{S}_w \end{bmatrix} < 0, \tag{33}$$

$$\mathbf{X}(t) \le \mathbf{S}^{-1}(t), \tag{34}$$

$$\mathbf{S}(t) = \mathbf{C}^T(t)\mathbf{S}_y(t)\mathbf{C}(t). \tag{35}$$

Then the system given by (26) and (27) is described by IO-FTS with respect to $(T, \mathbf{S}_w, \mathbf{S}_y(t))$ in the finite time interval $[0, T]$. The state feedback controller $\mathbf{u}(t) = \mathbf{K}(t)\bar{\mathbf{x}}(t)$, and $\mathbf{K}(t) = \mathbf{L}(t)\mathbf{X}^{-1}(t)$.

Proof. Let $\mathbf{V}(\mathbf{x}(t)) = \mathbf{x}^T(t)\mathbf{P}(t)\mathbf{x}(t)$, and then one has

$$\begin{aligned} \dot{\mathbf{V}} &= \frac{d}{dt}\left(\mathbf{x}^T\mathbf{P}\mathbf{x}\right) = \mathbf{x}^T\dot{\mathbf{P}}\mathbf{x} + \dot{\mathbf{x}}^T\mathbf{P}\mathbf{x} + \mathbf{x}^T\mathbf{P}\dot{\mathbf{x}} \\ &= \mathbf{x}^T\left(\dot{\mathbf{P}} + \mathbf{A}^T\mathbf{P} + \mathbf{P}\mathbf{A}\right)\mathbf{x} + \mathbf{w}^T\mathbf{G}^T\mathbf{P}\mathbf{x} + \mathbf{x}^T\mathbf{P}\mathbf{G}\mathbf{w}. \end{aligned} \tag{36}$$

(In the following proofs, one omits variable t for brevity.)

By (30) and (36), the inequality equation (37) can be derived.

$$\frac{d}{dt}\left(\mathbf{x}^T\mathbf{P}\mathbf{x}\right) < \mathbf{w}^T\mathbf{G}^T\mathbf{P}\mathbf{x} + \mathbf{x}^T\mathbf{P}\mathbf{G}\mathbf{w} - \mathbf{x}^T\mathbf{P}\mathbf{G}\mathbf{S}_w^{-1}\mathbf{G}^T\mathbf{P}\mathbf{x}. \tag{37}$$

Assume $\mathbf{v}(t)$ as the middle variable, and let $\mathbf{v}(t) = (\mathbf{S}_w^{1/2}\mathbf{w} - \mathbf{S}_w^{-1/2}\mathbf{G}^T\mathbf{P}\mathbf{x})$.

Then (38) can be obtained.

$$\mathbf{v}^T\mathbf{v} = \mathbf{w}^T\mathbf{S}_w\mathbf{w} + \mathbf{x}^T\mathbf{P}\mathbf{G}\mathbf{S}_w^{-1}\mathbf{G}^T\mathbf{P}\mathbf{x} - \mathbf{w}^T\mathbf{G}^T\mathbf{P}\mathbf{x} - \mathbf{x}^T\mathbf{P}\mathbf{G}\mathbf{w}. \tag{38}$$

According to (37) and (38), one can derive

$$\frac{d}{dt}\left(\mathbf{x}^T\mathbf{P}\mathbf{x}\right) < \mathbf{w}^T\mathbf{S}_w\mathbf{w} - \mathbf{v}^T\mathbf{v} < \mathbf{w}^T\mathbf{S}_w\mathbf{w}. \tag{39}$$

Integrating (39) from 0 to t, $t \in (0, T]$, and one has

$$\mathbf{x}(t)^T\mathbf{P}(t)\mathbf{x}(t) < \int_0^t \mathbf{w}(\tau)^T\mathbf{S}_\mathbf{w}\mathbf{w}(\tau)d\tau \le 1. \quad (40)$$

By (28), (31), (32), and (40), one can obtain

$$\mathbf{y}(t)^T\mathbf{S}_\mathbf{y}(t)\mathbf{y}(t) = \mathbf{x}(t)^T\mathbf{C}^T(t)\mathbf{S}_\mathbf{y}(t)\mathbf{C}(t)\mathbf{x}(t) < \mathbf{x}(t)^T\mathbf{P}(t)\mathbf{x}(t) < 1, \quad \text{for all } t \in [0, T]. \quad (41)$$

By using Schur complements [39], inequality equation (42) can be derived according to (30) and (41).

$$\begin{bmatrix} \dot{\mathbf{P}}(t) + \mathbf{A}^T(t)\mathbf{P}(t) + \mathbf{P}(t)\mathbf{A}(t) & \mathbf{P}(t)\mathbf{G}(t) \\ \mathbf{G}^T(t)\mathbf{P}(t) & -\mathbf{S}_\mathbf{w} \end{bmatrix} < 0. \quad (42)$$

Let $\mathbf{X}(t) = \mathbf{P}^{-1}(t)$, and one has $\dot{\mathbf{X}}(t) = -\mathbf{P}^{-1}(t)\dot{\mathbf{P}}(t)\mathbf{P}^{-1}(t)$. Multiply matrix inequality equation (42) by $\text{diag}\{\mathbf{P}^{-1}(t), \mathbf{I}\}$ on the right- and left-hand sides, and then the matrix inequality equation (43) can be derived.

$$\begin{bmatrix} -\dot{\mathbf{X}}(t) + \mathbf{X}(t)\mathbf{A}^T(t) + \mathbf{A}(t)\mathbf{X}(t) & \mathbf{G}(t) \\ \mathbf{G}^T(t) & -\mathbf{S}_\mathbf{w} \end{bmatrix} < 0. \quad (43)$$

By system equations (27) and (28), replace matrix $\mathbf{A}(t)$ by $\bar{\mathbf{A}}(t)$ in matrix inequality equation (43), and $\bar{\mathbf{A}}(t) = \mathbf{A}_1(t) + \mathbf{B}(t)\mathbf{K}(t)$.

Let $\mathbf{L}(t) = \mathbf{K}(t)\mathbf{X}(t)$, and then matrix inequality equation (33) can be deduced by simple replacement. Then one proves that matrix inequality equations (33), (34), and (35) can be obtained by transformation of matrix inequality (43), (31), and (32). Therefore, Theorem 2 is proven.

Remark 5. To determine the state feedback controller $\mathbf{u}(t)$, it is necessary to solve the differential linear matrix inequality (DLMI) equation, such as matrix inequality equation (33). The DLMI can be recast in term of several criteria linear matrix inequality equations, which is an appropriate method for solving a DLMI.

Remark 6. One discretizes DLMI into several standard LMIs, and the issue of controller design is transformed into the problem of solving LMIs. Based on the Matlab control toolbox and the in-point method, the numerical solution of LMIs can be calculated after several iteration loops. Therefore, the feasibility of the solution can be guaranteed by the existing method and software. The details for this procedure can be referred to in [39].

4. Simulation Analysis

In this section, a simulation analysis is conducted to evaluate the behavior of the multiple-aircraft cooperative intercept scenario. The specific process can be divided into two steps: (1) Based on the system state equations (25) and (26), the state feedback controller $\mathbf{u}(t)$ is designed based on the finite time controller design theory; (2) multiple-aircraft cooperative performance is examined using the closed-loop system.

Owing to the fact that the intercept angles of the Defenders and cooperative maneuvering of Evader can affect flight performance simultaneously, in Sections 4.1–4.3, we conduct three different simulation experiments to analyze their cooperative performance. The validity and stability of the cooperative guidance law are then verified for different initial launch conditions in Section 4.4.

4.1. Two Defenders Intercept Pursuer from One Side without Cooperation of Evader. In this case, Evader launches Defender 1 and Defender 2 for cooperative intercept, and Evader does not cooperate with Defender 1 and Defender 2. We assume that the two Defenders hit the Pursuer from the top for a better attack effect; therefore, the intercept angles of Defender 1 and Defender 2 are set to -15° and -30°, respectively. Based on the system equations derived in Section 2.2 and Section 2.4, the controller $\mathbf{u}(t)$ is solved based on Theorem 2. The simulation parameters are shown in Table 1.

Figure 3 presents the flight trajectory of the four aircraft without the cooperative maneuvering of Evader. It is apparent that the trajectory of Evader is relatively flat, and that Evader does not maneuver with Defenders for cooperative evasion. Pursuer attempts to attack Evader according to its guidance command. Evader launches Defender 1 and Defender 2 for cooperative intercept at the time 0 s. Defender 1 and Defender 2 cooperate with each other to intercept Pursuer from the same side.

Figure 4 shows the variation of the interception angles, with the intercept angles of Defender 1 and Defender 2 controlled at -15° and -30° during the terminal guidance period.

Figure 5 shows the variation of the LOS angle rotation rate. The simulation results show that the LOS angle rotation rates of Defender 1 and Defender 2 finally converge to zero, indicating that the Defenders can intercept Pursuer in the case of positive approaching speed.

The above simulation results support the conclusion that the Defenders accomplish the cooperative interception in the finite time interval, showing that the designed controller can guarantee the ability of the Defenders to cooperatively intercept at preassigned angles. Thus, the theoretical methods underpinning the controller design are verified.

In order to illustrate the effectiveness and advantages of the guidance law proposed in this paper, we conduct a comparative simulation experiment. Two defenders use the proposed guidance law and the augmented proportional navigation (APN, $N = 5$, $K = 2$) with angle restraints in [17], respectively. Evader does not cooperate with Defender 1 and Defender 2. The intercept angles of Defender 1 and Defender 2 are set to -15° and -30°, respectively. The remaining parameters are the same as those given in Table 1.

The simulation results are shown in Figures 6–8. By Figures 6–8, the trajectory of the proposed guidance law is more gentle than that of the APN with the same interception angle constraints and initial conditions, which indicates that the proposed guidance law can effectively reduce the required acceleration of the defenders. The acceleration requirement shown in Figures 7 and 8 also verifies the conclusion in Figure 6. These simulation results confirm the usefulness

Table 1: Simulation parameters for cooperative intercept.

Parameter	Symbol	Initial value
Initial range	$r_{PE}(0)$	15,000 m
Initial range	$r_{PD1}(0), r_{PD2}(0)$	15,000 m
Velocity of Evader	V_E	250 m/s
Velocity of Pursuer	V_P	500 m/s
Velocity of Defenders	V_{D1}, V_{D2}	500 m/s
Response time of Evader	τ_E	0.1 s
Response time of Defenders	τ_{D1}, τ_{D2}	0.05 s
Response time of Pursuer	τ_P	0.05 s
Navigation parameter	N	4
Navigation parameter	K	3
Initial system state vector	$\mathbf{x}(0)$	$[0 \quad 0 \quad 0 \quad 0.05 \quad -0.02 \quad -0.03 \quad 0 \quad 0 \quad 0 \quad 0]^T$
Measurement matrix function	$\mathbf{S}_y(\cdot)$	$950t \cdot \mathbf{I}_{4\times4}$
Measurement matrix	$\mathbf{S}_w$	$\mathbf{I}_{1\times1}$

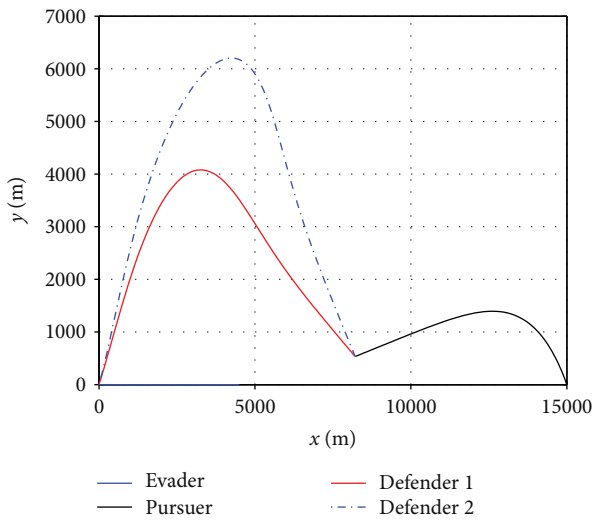

Figure 3: Four aircraft flight trajectories (one-side intercept without cooperation of Evader).

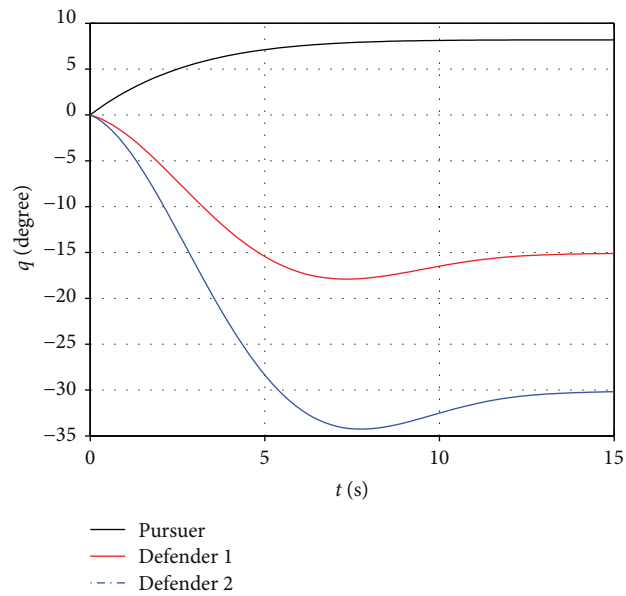

Figure 4: Intercept angle variation of the aircraft.

and advantages of the proposed guidance law in this paper when compared with other guidance law.

4.2. Two Defenders Intercept Pursuer from One Side with the Cooperation of Evader. In this case, based on the system state equations derived in Section 2.3 and Section 2.4, the controller $\mathbf{u}(t)$ is solved by Theorem 2. Unlike in Section 4.1, Evader cooperates with the Defenders to improve intercept performance. The interception angles of Defender 1 and Defender 2 are set to -15° and -30°, respectively. The remaining parameters are the same as those given in Table 1.

Figure 9 presents the flight trajectories of the four aircraft for the condition of cooperative maneuver of Evader. It is apparent that Evader maneuvers with Defenders to perform a collaborative defense, allowing Defender 1 and Defender 2 to intercept Pursuer together at their preassigned intercept angles.

Figure 10 indicates that intercept angles of Defender 1 and Defender 2 converge to -15° and -30° in the final phase. Figure 11 shows the change of the LOS angle rotation rate with the cooperation of Evader. By Figures 9–11, it can be concluded that the Defenders successfully intercept Pursuer at a preassigned intercept angle with the cooperation of Evader.

Comparing the accelerations of Defender 1 and Defender 2 in the cooperation and noncooperation scenarios presented in Cases A and B, respectively, we can obtain the comparative accelerations illustrated in Figures 12 and 13. The simulation results prove that for the one-side intercept

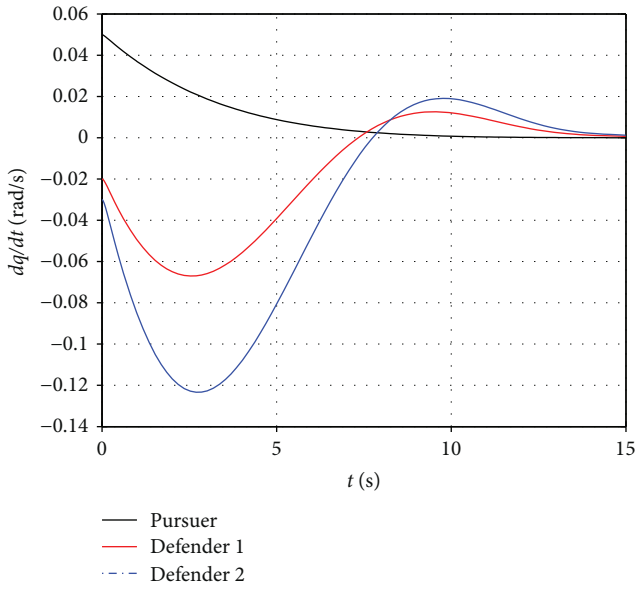

Figure 5: The variation of LOS angle rotation rate.

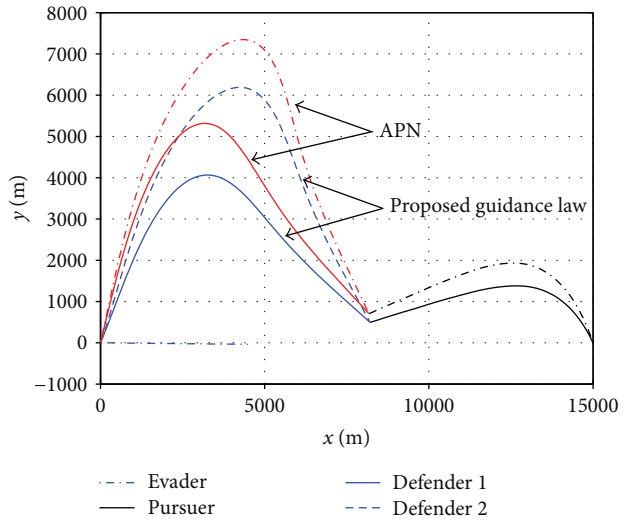

Figure 6: Four aircraft flight trajectories.

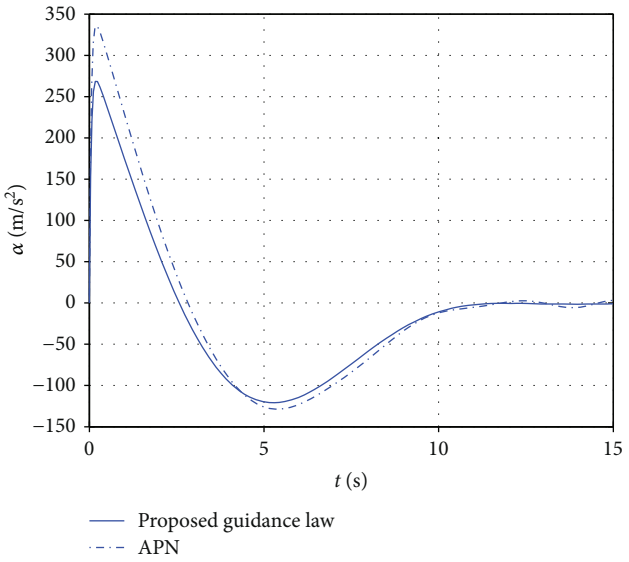

Figure 7: The acceleration variation of Defender 1.

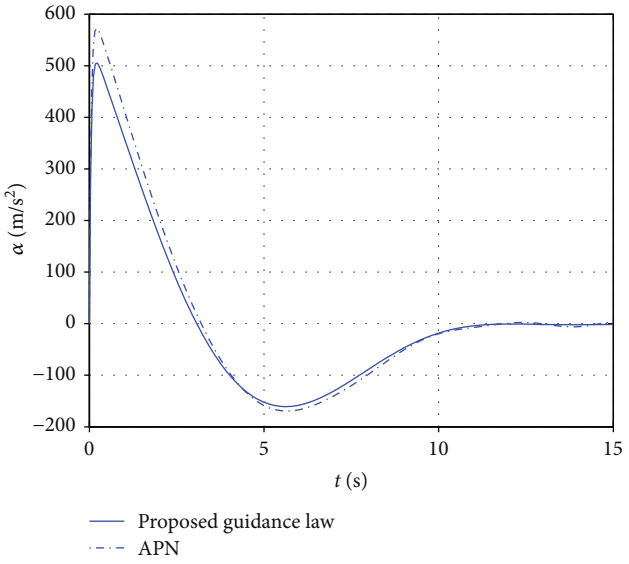

Figure 8: The acceleration variation of Defender 2.

scenarios, cooperative guidance with the cooperation of Evader can significantly reduce the maximum required acceleration for both Defenders. The Defenders achieve a better intercept performance by pursuing different intercept angles in cooperation with the maneuvers of Evader. These simulation results confirm the usefulness and advantages of cooperation for both Defenders.

4.3. Two Defenders Intercept Pursuer from Two Sides with Cooperation of Evader. From the point of view of probability, if the Defenders attempt to intercept Pursuer from two sides, it will be more difficult for Pursuer to avoid the interception [2, 12]. The two-side cooperative intercept case is expected to present a more effective collaborative defense for Evader. Therefore, in this case, the Defenders use a two-side intercept mode to increase the intercept probability, setting the intercept angles of the Defenders to 30° and −30°. Additionally, Evader cooperates with its defense in the cooperative interception. The initial value of the state vector is $\mathbf{x}(0) = [0 \quad 0 \quad 0 \quad 0.05 \quad 0.03 \quad -0.03 \quad 0 \quad 0 \quad 0 \quad 0]^{\mathrm{T}}$. The remaining parameters are the same as those given in Table 1. Based on the system state equations derived in Section 2.3 and Section 2.4, we can design the cooperative guidance law $\mathbf{u}(t)$.

Figure 14 shows the flight trajectory of the four aircraft without the cooperation of Evader. Figure 15 shows the flight trajectory of the four aircraft with the cooperation of Evader. The comparison of Figures 14 and 15 indicates that Evader substantially cooperates with the Defenders in cooperative evasion.

Figures 16 and 17 reveal the variation of intercept angles and LOS angle rotation rates with the cooperation of Evader.

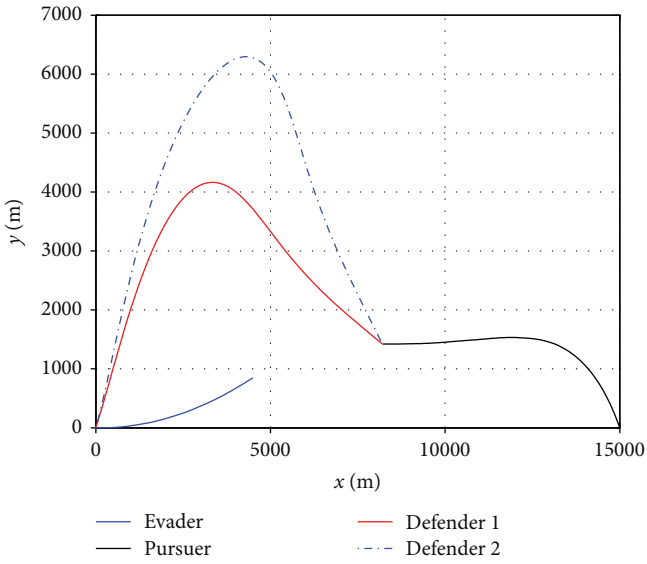

Figure 9: Four aircraft flight trajectories (one-side intercept with cooperation of Evader).

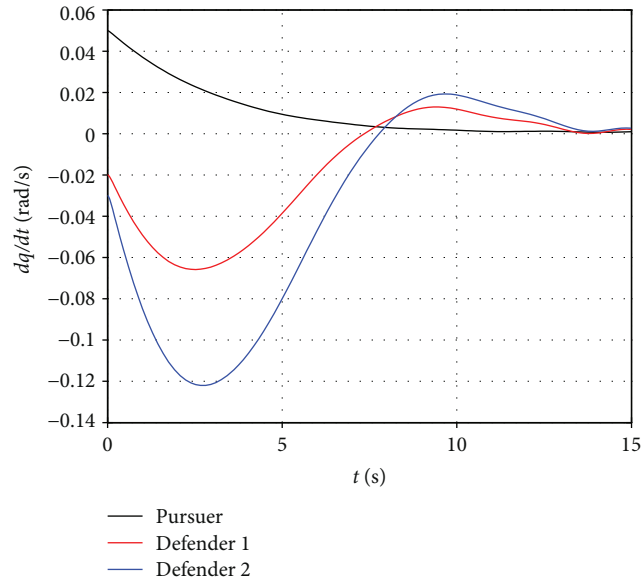

Figure 11: LOS angle rotation rate variation.

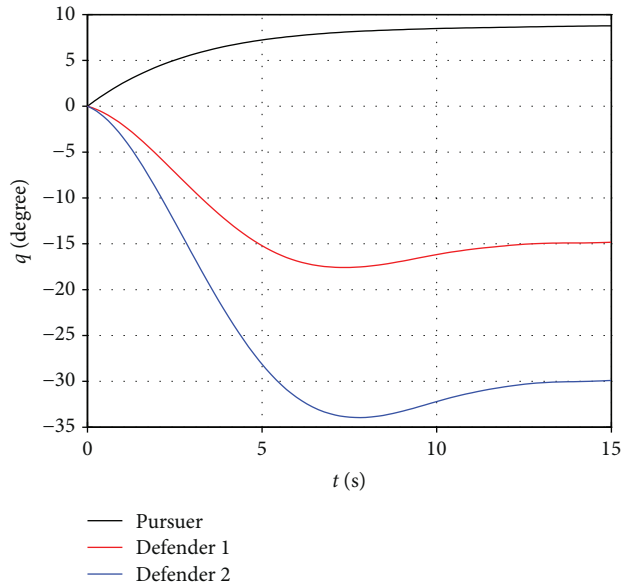

Figure 10: Intercept angle variation of the aircraft.

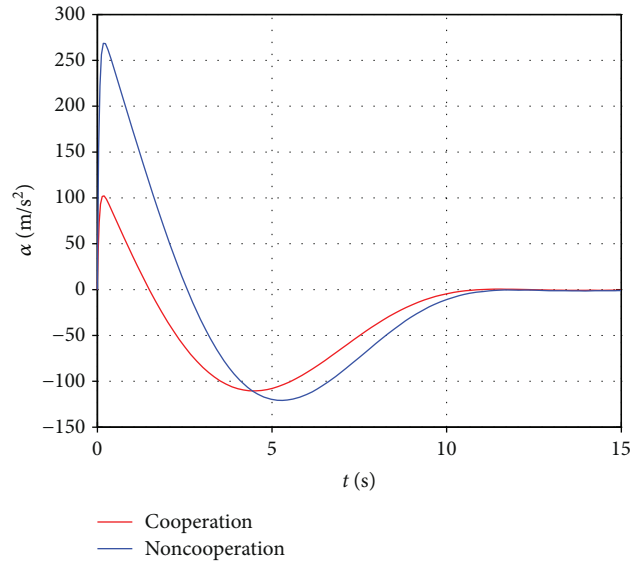

Figure 12: Acceleration variation of Defender 1 (one-side intercept).

By Figures 15–17, it can be concluded that the Defenders can collaboratively intercept Pursuer at predetermined interception angles from both sides.

Figures 18 and 19 show the compared results of acceleration in the two-side intercept case. In the case of the noncooperation of Evader, the maximum required acceleration for the Defender 2 reaches 403.5 m/s^2, and that of Defender 1 reaches 338.4 m/s^2, indicating that compared with Defender 1, Defender 2 is more difficult to maneuver for successful intercept. Consequently, the simulation results indicate that for the two-side cooperative intercept case, Evader tends to cooperate more with the defender who demands a greater required acceleration, illustrating that the cooperative intercept scenario can reduce the required acceleration of the defender with whom Evader cooperates.

4.4. Performance Analysis under Different Initial Launch Conditions. The initial launch conditions of the Defenders may be affected by the various flying situations of Evader. Additionally, while engaging with the different requirements of the combat mission, the Defenders must confront different battlefield launch conditions in which the validity and stability of the guidance law is critical to ensure accurate attack. Based on the cooperative guidance law proposed in Section 3, in this section, the performance analysis of the cooperative guidance law is conducted under different initial launch

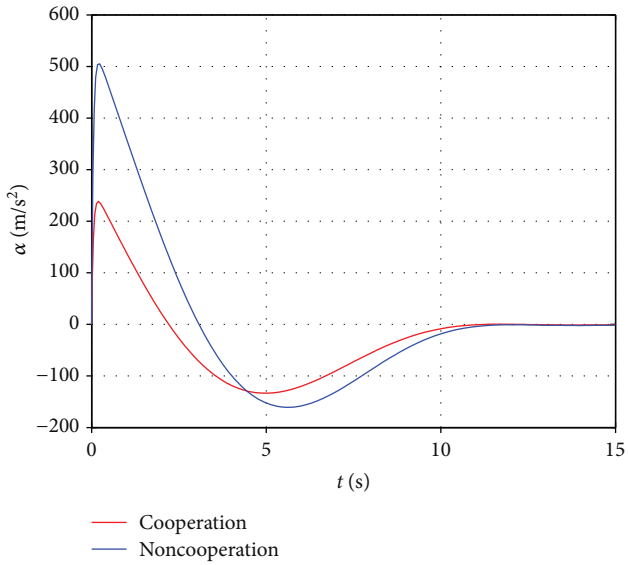

Figure 13: Acceleration variation of Defender 2 (one-side intercept).

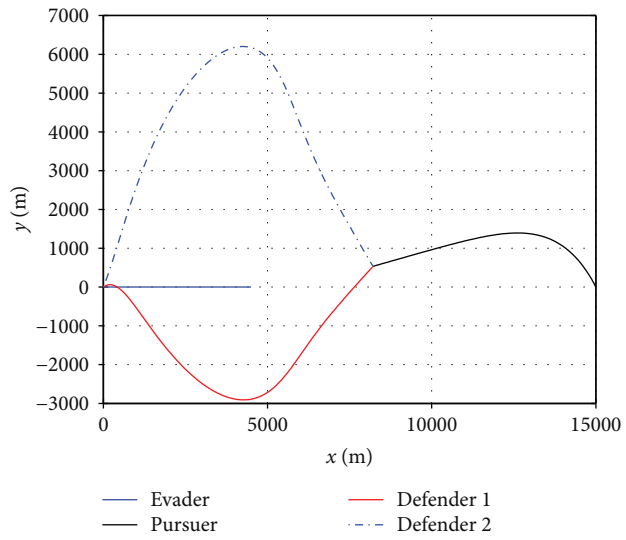

Figure 14: Four aircraft flight trajectories (two-side intercept without cooperation of Evader).

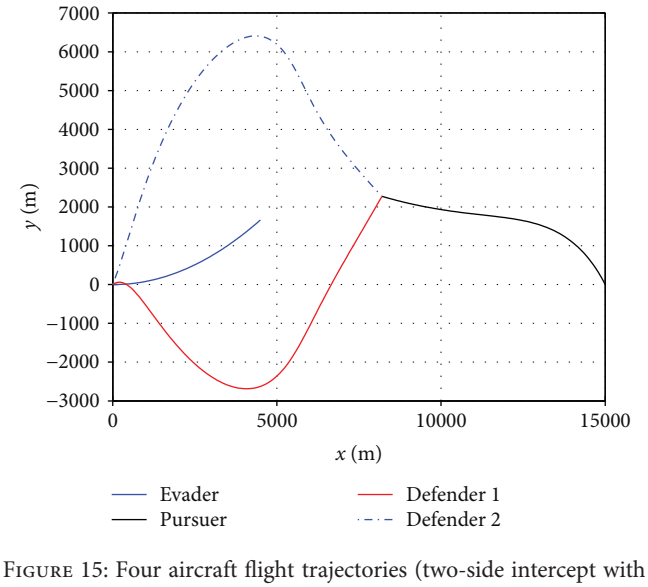

Figure 15: Four aircraft flight trajectories (two-side intercept with cooperation of Evader).

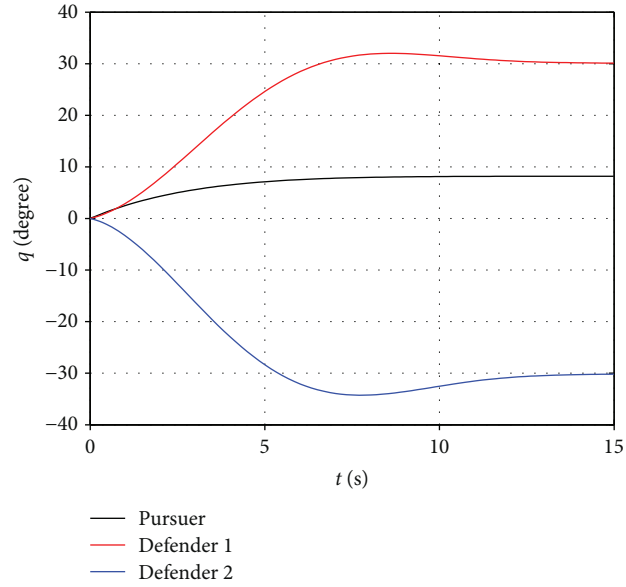

Figure 16: Intercept angle variation of the aircraft.

conditions. When the Defenders are separated from Evader, the different launch conditions will ultimately affect the initial LOS angular rate $\dot{q}_i$, $i = \{\text{PD1}, \text{PD2}\}$.

The simulation scenario is set up as follows: Evader cooperates with the two Defenders for cooperative evasion, and Defender 1 and Defender 2 intercept the Pursuer from different sides. The intercept angle of Defender 1 is set to 30°, and the intercept angle of Defender 2 is set to −30°. The initial value of the LOS angle rotation rate $\dot{q}$ is set differently for five cases, shown in Table 2. The remaining parameters are the same as those given in Table 1.

Figures 20 and 21 show the variation of the intercept angles of Defender 1 and Defender 2, respectively, in the five considered cases. Figures 22 and 23 show the variation of the LOS angle rotation rates $\dot{q}_{\text{PD1}}$ and $\dot{q}_{\text{PD2}}$ for the two Defenders in the five considered cases. As can be seen from these figures, Defender 1 and Defender 2 have the ability to intercept Pursuer at preassigned intercept angles under all five different initial launch conditions. The intercept angles eventually converge to 30° and −30°, and the LOS angle rotation rates $\dot{q}_{\text{PD1}}$ and $\dot{q}_{\text{PD2}}$ eventually converge to 0 rad/s, despite the variation in initial launch conditions. These simulation results verify the effectiveness of the proposed cooperative guidance law. Moreover, these simulations also demonstrate the strong adaptability and robustness of the proposed guidance law under various initial launch conditions.

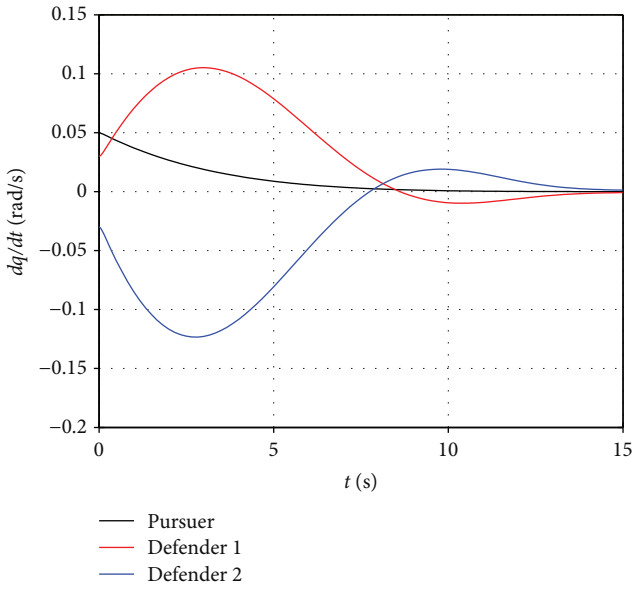

Figure 17: LOS angle rotation rate variation.

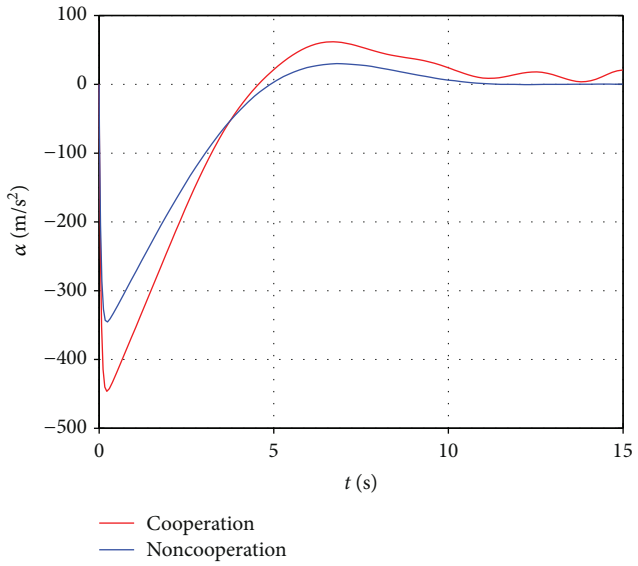

Figure 18: Acceleration variation of Defender 1 (two-side intercept).

5. Conclusions

This study focuses on a four-aircraft intercept engagement scenario. Compared with previous research, this study primarily addresses two novel aspects of the intercept engagement scenario: (1) the cooperative intercept performance analysis of multiple defenders under intercept angle constraints and (2) the cooperative intercept performance analysis of the aircraft with the cooperation of the Evader in a lure role. Based on the relative motion and kinetic equations of the four-aircraft cooperative intercept models, three different cases of engagement are established. The design method for the state feedback controller is proposed based on the input and output finite time stability theory and is applied in the

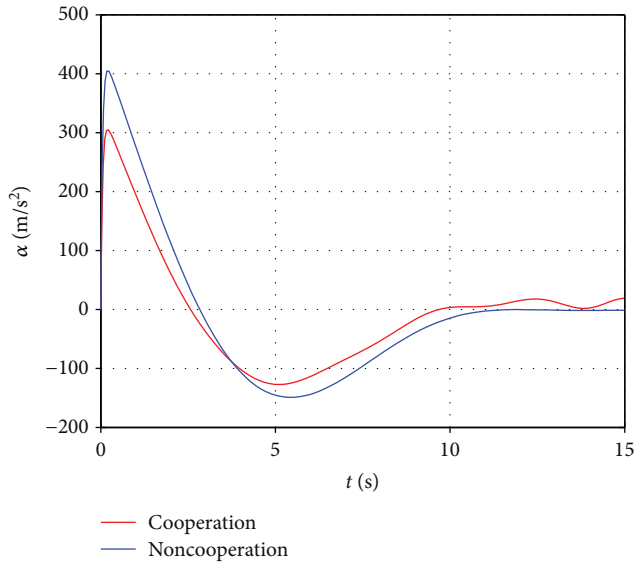

Figure 19: Acceleration variation of Defender 2 (two-side intercept).

Table 2: Initial launch parameters of the two Defenders.

Case	Initial value $\dot{q}_{PD1}$ (rad/s)	Initial value $\dot{q}_{PD2}$ (rad/s)
1	0.01	−0.01
2	0.03	−0.03
3	0.06	−0.06
4	0.09	−0.09
5	0.1	−0.1

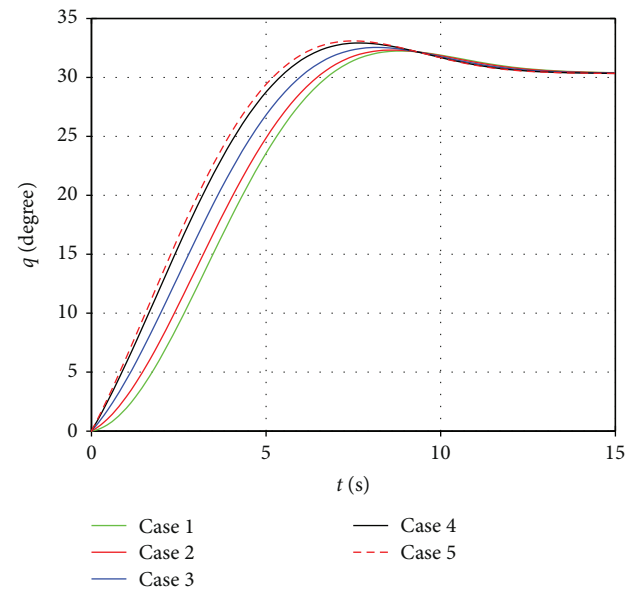

Figure 20: Intercept angle variation of Defender 1.

controller solution for the four-aircraft engagement. The simulation results show that the proposed method can guarantee that Defender 1 and Defender 2 intercept Pursuer at

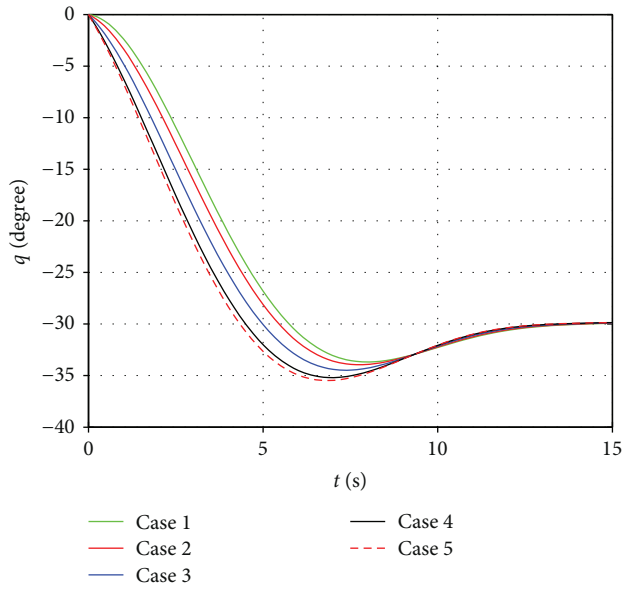

Figure 21: Intercept angle variation of Defender 2.

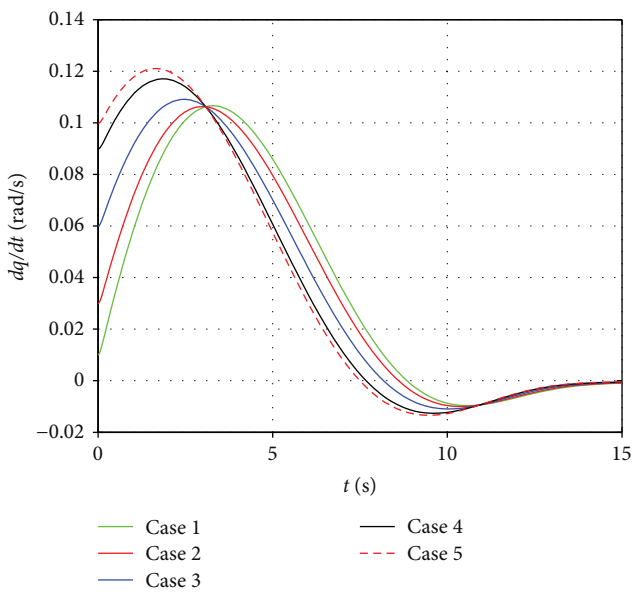

Figure 22: LOS angle rotation rate variation of Defender 1.

the preassigned intercept angles, and that the Defenders can achieve improved interception performance with the cooperation of Evader. It was also shown that the two Defenders can intercept Pursuer from either the same side or both sides, as a function of the desired intercept angle. The one-side cooperative intercept scenario reduces the maximum required acceleration of both defenders, while the two-side cooperative intercept scenario increases the intercept probability. When cooperating with the Defenders in a two-sided interception scenario, Evader tends to cooperate more with the defender who demands a greater required acceleration. Finally, the simulations demonstrate that the proposed cooperative guidance law possesses strong adaptability and robustness in the face of different initial launch conditions.

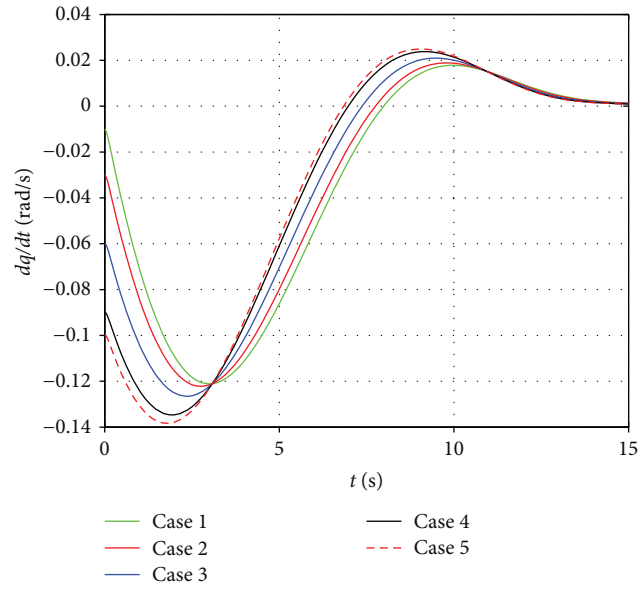

Figure 23: LOS angle rotation rate variation of Defender 2.

Nomenclature

a_i:	Normal acceleration of vehicle i (m/s^2)
a_{iC}:	Normal acceleration command (m/s^2)
A, **B**, **C**, **G**:	State-space representations of the dynamics
$\mathbf{A}_1(t)$:	The augmented system state matrix
D1, D2:	Defender 1 and Defender 2
E:	Evader
$\mathbf{K}(t)$:	The state feedback matrix
N, K:	The augmented proportional navigation parameters
P:	Pursuer
P, **X**, **L**:	Symmetric positive definite matrix-valued function
q_{ij}:	LOS angle from the vehicle i to the vehicle j (rad)
$\dot{q}_{ij}$:	LOS angle rotation rate from the vehicle i to the vehicle j (rad/s)
$r_{ij}(t)$:	Range between the vehicle i to the vehicle j (m)
$r_{ij}(0)$:	Initial range between the vehicle i to the vehicle j (m)
$\mathbf{S}_w$:	Measurement matrix
$\mathbf{S}_y(t)$:	Measurement matrix function
t_f:	The total flight time (s)
T:	Positive time scalar
$\mathbf{u}(t)$:	System control input vector
V:	Velocity (m/s)
$\mathbf{w}(t)$:	System external input vector
$\mathbf{x}(t)$:	System state variables
$\mathbf{x}(0)$:	The initial system state variables
$\bar{\mathbf{x}}(t)$:	The augmented system state variables
$\mathbf{y}(t)$:	System evaluation output vector
$\bar{\mathbf{y}}(t)$:	The augmented system evaluation output vector
τ_i:	Dynamic response time constants of the vehicle i (s)
$\boldsymbol{\delta}$:	The augmented vector of system state, $\boldsymbol{\delta} \in \mathbb{R}^{10}$.

Conflicts of Interest

The authors declare that there is no conflict of interests regarding the publication of this paper.

Acknowledgments

This work was supported by the National Natural Science Foundation (NNSF) of China under grant number 61673386 and the Aviation Foundation of China under grant number 201651U8006.

References

[1] V. Shaferman and T. Shima, "Cooperative optimal guidance laws for imposing a relative intercept angle," in *AIAA Guidance, Navigation, and Control Conference*, pp. 4909–4923, Minnesota, MN, USA, 2012.

[2] V. Shaferman and T. Shima, "Cooperative optimal guidance laws for imposing a relative intercept angle," *Journal of Guidance, Control, and Dynamics*, vol. 38, no. 8, pp. 1395–1408, 2015.

[3] R. L. Boyell, "Defending a moving target against missile or torpedo attack," *IEEE Transactions on Aerospace and Electronic Systems*, vol. AES-12, no. 4, pp. 522–526, 1976.

[4] R. L. Boyell, "Counterweapon aiming for defense of a moving target," *IEEE Transactions on Aerospace and Electronic Systems*, vol. AES-16, no. 3, pp. 402–408, 1980.

[5] T. Shima, "Optimal cooperative pursuit and evasion strategies against a homing missile," *Journal of Guidance, Control, and Dynamics*, vol. 34, no. 2, pp. 414–425, 2011.

[6] O. Prokopov and T. Shima, "Linear quadratic optimal cooperative strategies for active aircraft protection," *Journal of Guidance, Control, and Dynamics*, vol. 36, no. 3, pp. 753–764, 2013.

[7] M. Weiss, T. Shima, and D. Castaneda, "Combined and cooperative minimum-effort guidance algorithms in an active aircraft defense scenario," *Journal of Guidance, Control, and Dynamics*, vol. 40, no. 5, pp. 1241–1254, 2017.

[8] T. Yamasaki and S. N. Balakrishnan, "Triangle intercept guidance for aerial defense," in *AIAA Guidance, Navigation, and Control Conference*, pp. 2010–7876, Toronto, Canada, 2010.

[9] A. Ratnoo and T. Shima, "Line-of-sight interceptor guidance for defending an aircraft," *Journal of Guidance, Control, and Dynamics*, vol. 34, no. 2, pp. 522–532, 2011.

[10] Y. Guo, X. Hu, F. He, H. Cheng, and Q. Gao, "Triangle interception scenario: a finite-time guidance approach," *International Journal of Aerospace Engineering*, vol. 2016, Article ID 2942686, 12 pages, 2016.

[11] Y. Guo, Y. Yao, S. Wang, B. Yang, F. He, and P. Zhang, "Maneuver control strategies to maximize prediction errors in ballistic middle phase," *Journal of Guidance, Control, and Dynamics*, vol. 36, no. 4, pp. 1225–1234, 2013.

[12] V. Shaferman and T. Shima, "A cooperative differential game for imposing a relative intercept angle," in *AIAA Guidance, Navigation, and Control Conference*, pp. 1015–1040, Grapevine, TX, USA, 2017.

[13] R. Fonod and T. Shima, "Estimation enhancement by cooperatively imposing relative intercept angles," *Journal of Guidance, Control, and Dynamics*, vol. 40, no. 7, pp. 1711–1725, 2017.

[14] R. Fonod and T. Shima, "Estimation enhancement by imposing a relative intercept angle for defending missiles," in *AIAA Guidance, Navigation, and Control Conference*, pp. 1018–1032, Grapevine, TX, USA, 2017.

[15] H. Du and S. Li, "Attitude synchronization for flexible spacecraft with communication delays," *IEEE Transactions on Automatic Control*, vol. 61, no. 11, pp. 3625–3630, 2016.

[16] S. Li, H. Du, and P. Shi, "Distributed attitude control for multiple spacecraft with communication delays," *IEEE Transactions on Aerospace and Electronic Systems*, vol. 50, no. 3, pp. 1765–1773, 2014.

[17] Y. Zhang, X. Wang, and H. Wu, "A distributed cooperative guidance law for salvo attack of multiple anti-ship missiles," *Chinese Journal of Aeronautics*, vol. 28, no. 5, pp. 1438–1450, 2015.

[18] A. Ratnoo and T. Shima, "Guidance strategies against defended aerial targets," *Journal of Guidance, Control, and Dynamics*, vol. 35, no. 4, pp. 1059–1068, 2012.

[19] N. Balhance, M. Weiss, and T. Shima, "Cooperative guidance law for intrasalvo tracking," *Journal of Guidance, Control, and Dynamics*, vol. 40, no. 6, pp. 1441–1456, 2017.

[20] S. R. Kumar and T. Shima, "Cooperative nonlinear guidance strategies for aircraft defense," *Journal of Guidance, Control, and Dynamics*, vol. 40, no. 1, pp. 124–138, 2017.

[21] Y. Guo, S. Wang, Y. Yao, and B. Yang, "Evader maneuver on consideration of energy consumption in flight vehicle interception scenarios," *Aerospace Science and Technology*, vol. 15, no. 7, pp. 519–525, 2011.

[22] Y. Guo, Y. Yao, S. Wang, B. Yang, K. Liu, and X. Zhao, "Finite-time control with H-infinity constraints of linear time-invariant and time-varying systems," *Journal of Control Theory and Applications*, vol. 11, no. 2, pp. 165–172, 2013.

[23] Y. Guo, Y. Yao, S. Wang, K. Ma, K. Liu, and J. Guo, "Input-output finite-time stabilization of linear systems with finite-time boundedness," *ISA Transactions*, vol. 53, no. 4, pp. 977–982, 2014.

[24] H. Du, C. Qian, S. Yang, and S. Li, "Recursive design of finite-time convergent observers for a class of time-varying nonlinear systems," *Automatica*, vol. 49, no. 2, pp. 601–609, 2013.

[25] M. Golestani, I. Mohammadzaman, and A. R. Vali, "Finite-time convergent guidance law based on integral backstepping control," *Aerospace Science and Technology*, vol. 39, no. 5, pp. 370–376, 2014.

[26] M. Golestani and I. Mohammadzaman, "PID guidance law design using short time stability approach," *Aerospace Science and Technology*, vol. 43, no. 6, pp. 71–76, 2015.

[27] P. Dorato, "Short-time stability in linear time-varying systems," in *Proceedings of the IRE International Convention Record Part 4*, pp. 83–87, New York, NY, USA, 1961.

[28] S. P. Bhat and D. S. Bernstein, "Finite-time stability of continuous autonomous systems," *SIAM Journal on Control and Optimization*, vol. 38, no. 3, pp. 751–766, 2000.

[29] Y. Hong, Z. P. Jiang, and G. Feng, "Finite-time input-to-state stability and applications to finite-time control," *IFAC Proceedings Volumes*, vol. 41, no. 2, pp. 2466–2471, 2008.

[30] H. Du, G. Wen, Y. Cheng, Y. He, and R. Jia, "Distributed finite-time cooperative control of multiple high-order nonholonomic mobile robots," *IEEE Transactions on Neural Networks and Learning Systems*, vol. 28, no. 12, pp. 2998–3006, 2017.

[31] S. Li, H. Du, and X. Lin, "Finite-time consensus algorithm for multi-agent systems with double-integrator dynamics," *Automatica*, vol. 47, no. 8, pp. 1706–1712, 2011.

[32] J. X. Xi, M. He, H. Liu, and J. F. Zheng, "Admissible output consensualization control for singular multi-agent systems with time delays," *Journal of the Franklin Institute*, vol. 353, no. 16, pp. 4074–4090, 2016.

[33] J. X. Xi, Z. L. Fan, H. Liu, and T. Zheng, "Guaranteed-cost consensus for multi agent networks with Lipschita nonlinear dynamics and switching topologies," *International Journal of Robust and Nonlinear Control*, pp. 1–12, 2018.

[34] F. Amato, M. Ariola, and P. Dorato, "Finite-time control of linear systems subject to parametric uncertainties and disturbances," *Automatica*, vol. 37, no. 9, pp. 1459–1463, 2001.

[35] F. Amato, R. Ambrosino, C. Cosentino, and G. de Tommasi, "Input-output finite time stabilization of linear systems," *Automatica*, vol. 46, no. 9, pp. 1558–1562, 2010.

[36] F. Amato, G. Carannante, G. De Tommasi, and A. Pironti, "Input-output finite-time stability of linear systems: necessary and sufficient conditions," *IEEE Transactions on Automatic Control*, vol. 57, no. 12, pp. 3051–3063, 2012.

[37] F. Amato, R. Ambrosino, M. Ariola, C. Cosentino, and G. De Tommasi, *Finite-time stability and control*, vol. 453 of Lecture Notes in Control and Information Sciences, Springer, London, UK, 2014.

[38] F. Amato, G. De Tommasi, and A. Pironti, "Necessary and sufficient conditions for input-output finite-time stability of impulsive dynamical systems," in *2015 American Control Conference (ACC)*, pp. 5998–6003, Chicago, IL, USA, 2015.

[39] U. Shaked and V. Suplin, "A new bounded real lemma representation for the continuous-time case," *IEEE Transactions on Automatic Control*, vol. 46, no. 9, pp. 1420–1426, 2001.